IOP Conf. Series: Journal of Physics: Conf. Series **830** (2017) 012158 doi:10.1088/1742-6596/830/1/012158

# Self-trapped exciton configurations in Beryllium Oxide

**M A Botov[1], A Yu Kuznetsov[2] and A B Sobolev[1]**

[1]Dept. of High Mathematics, Ural Federal University, 19 Mira St., Yekaterinburg, Russia
[2]Dept. of Experimental Physics, Ural Federal University, 19 Mira St., Yekaterinburg, Russia

**Abstract.** The modern radiation technology, nuclear engineering, non-linear optics are associated with radiation-resistant optical material study. Evolution of electronic excitations in these materials is a complex multichannel process which currently has no integrated model. A special role belongs to the low-symmetry single crystals, such as beryllium oxide (BeO). We present theoretical results that advance our understanding of exciton-based channel of electronic excitations relaxation. The four possible self-trapped exciton (STE) configurations in beryllia single crystal have been investigated by using a quantum mechanical approach (Hartree-Fock and B3LYP HF-DFT hybrid functional, as implemented in the CRYSTAL09 code). B3LYP DFT functional with 30% of exact exchange was used (B3LYP30). All calculations were performed using periodic boundary conditions and full SC geometry relaxation. The lattice distortion and charge density distribution for considered defect configurations were obtained. STE-A1 luminescence energy was found to be 6.0 eV for HF and 6.5 eV for B3LYP30; STE-A2 luminescence energy was found to be 9.2 eV for HF and 7.8 eV for B3LYP30. STE-B1 luminescence energy was found to be 5.5 eV for HF, 6.2 eV for B3LYP30; STE-B2 luminescence energy was found to be 4.7 eV for HF.

## 1. Introduction

The exciton is well known as a bound state of an electron and a hole which are attracted to each other by the electrostatic Coulomb force [1]. It can be trapped at a lattice distortion and in this case become self-trapped exciton (STE). Such STEs recombine to the ground state, producing a characteristic luminescence. STE in oxides have a long history of study. Nevertheless, a generally accepted theory of excited state formation and STE models in wide-gap oxide crystals does not still exist. It is well established that exciton self-trapping takes place only in low symmetry oxide crystals, such as $SiO_2$, $Al_2O_3$, $Y_2O_3$ [2,3,4]. STE luminescence bands were also detected in BeO [5,6,7]. Beryllia has a wide range of applications, it is the only material apart from diamond which combines high thermal-shock resistance, high electrical resistivity, and high thermal conductivity at a similar level. It is very promising for personal dosimetry due to the proximity of its effective atomic number (Z=7.13) to biological tissue (Z=7.42) [8]. Theoretical investigation of intrinsic Schottky and Frenkel defects in beryllia by means of molecular statics method was performed in [9]. However, the absence of ab initio quantum-mechanical calculations of STE in BeO still occurs. In this paper, we shall present such ab initio modeling of STE in beryllium oxide.

## 2. Model and calculation details

Our study is based on ab initio calculations performed in CRYSTAL09 [10] package using Hartree-Fock (HF) approximation and density functional theory functional B3LYP[11,12] with 30% of exact

exchange (B3LYP30). Atoms were described by their full-electron basis set (5-11G for Be and 8-411G for O)[13,14] with optimized valence shells. All calculations were performed using periodic boundary conditions and full supercell(SC) geometry relaxation. 108-atom supercell (symmetry group P63mc) was constructed as 3 × 3 × 3 expansions of BeO unit cell. A Monkhorst-Pack mesh of 13 k points in the irreducible part of the Brillouin zone was used for integration in the reciprocal space. Anderson's method [15] of Fock matrix mixing was used for better convergence. Our way to the stable STE model consists of two stages: the first is to model a hole and the second is to model STE itself. In the first stage, we place a hole at oxygen atom most remote from SC borders (by removing one electron from its outer shell). To facilitate initial hole localization, a small distortion at hole lattice site was created (such technique was inspired by [16,17,18]). An oxygen carrying hole was shifted up on 10% of lattice constant a (0.3 Å) along z axis. After that, SC geometry optimization procedure was performed. Shifting along x axis was also checked, but the result for z axis is energetically more favourable. The second stage was devoted to STE modelling. A peculiarity of STE structure is presence of two unpaired electrons; one of them belongs to an oxygen representing hole core, and another is localized in interatomic spacing near the hole (and we have to lock their spins to 1 during the calculation and use spin-unrestricted calculation schemes – UHF and corresponding DFT modification). Electron of STE is described by one diffuse Gauss-type s-orbital. This approach was earlier successfully applied for modelling of STE in alkali-halides [19] and corundum crystal [20]. Optimized values of exponent α-parameter in STE electron wave function are shown in Table 4. The final results after full SC geometry relaxation routine are discussed in the following section.

## 3. Results

The perfect BeO crystal parameters were calculated at the very first step in order to check basis sets correctness. The results are presented in Table 1. The results provided by B3LYP30 method are close to experimental data. HF typically overestimates energy gap.

**Table 1.** Calculated lattice constants *a*, *c* and internal parameter *z* (in Å), *a/c* ratio and energy gap Eg (in eV) of perfect BeO in comparison with experiment.

| Parameter | HF | B3LYP30 | Exp. |
|---|---|---|---|
| ***a*, Å** | 2.692 | 2.702 | 2.698[21] |
| ***c*, Å** | 4.336 | 4.369 | 4.380[21] |
| ***c*/*a*, Å** | 1.611 | 1.617 | 1.624[22] |
| **z, Å** | 0.384 | 0.377 | 0.378[22] |
| **Eg, eV** | 18.99 | 10.88 | 10.59[21] |

### *3.1. Configurations of STE*

Four off-centre STE configurations were studied. We denote them in terms of STE electron density center localization inside beryllium-oxygen tetrahedron: as "in(z)" (e inside tetrahedron, z-oriented) and "out(z)" (e outside tetrahedron, z-oriented), "in(x)" (e inside tetrahedron, initially x-oriented) and "out(x)" (e outside tetrahedron, initially x-oriented). We used 108 atoms supercell for both HF and B3LYP30 methods. Rather large SC is needed due to the size of the defect, delocalized character of its electronic component and defect-defect interactions between nearby SC. Figure 1 shows geometric structure and spin localization of mentioned configurations. It could be seen, that STE hole core is localized at one oxygen atom (O76 at Table.2 and Table.3). STE has shown itself as rather extensive formation – the distance between STE electron density center and O76 occupied by hole is about 50% of lattice constant a for axial orientation ("in(z)": 50.8% for HF and 47.6% for B3LYP30; "out(z)": 54.0% for HF and 61.5% for B3LYP30) and about 60% of a for non-axial orientation ("in(x)": 59% for HF and 58% for B3LYP30, "out(x)": 60% for HF). STE-"in" configurations are more compact than

STE-"out" ones. B3LYP30 give a 1% less size for STE_in(x) than HF. Unfortunately, B3LYP30 did not give stable solution corresponding to STE_out(x) configuration.

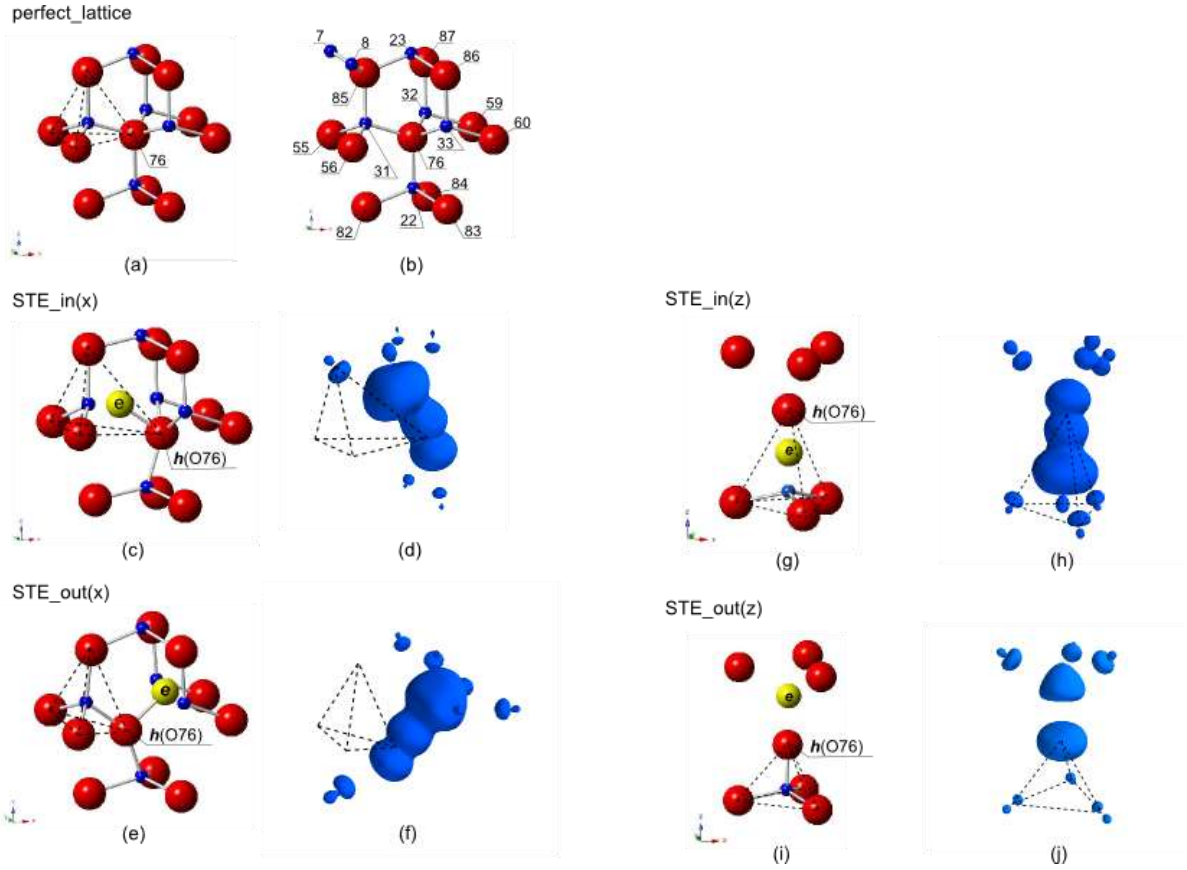


**Figure 1.** (Color online) Spin localization in the STE_in(x) and STE_out(x) configurations in BeO. Oxigens are red, Be-atoms are gray. Fictive atom "e" #109 (yellow) denotes location of STE electron density center. Fragments (a), (b), (c), (e), (g), (i) show the lattice around STE site and tetrahedron of interest. Fragments (d), (f), (h), (j) show the surface of the constant spin density with value S = 0.07.

It should be noted, that in spite of initial horizontal orientation of non-axial STE, after SC geometric relaxation STE become rotated around y-axis (sill laying in xz-plane). The final deviation from xy-plane reaches 35.5° for "in(x)" by HF, 35.9° for "in(x)" by B3LYP30 and 40.8° for "out(x)" by HF. STE appearance causes strong distortions of the surrounding lattice, especially at first coordination sphere.

*3.2. Relaxation*

Figure 1 (c), (e), (g) and (i) show STE surrounding atoms after geometry relaxation. Numbers of these atoms in SC are given at figure 1 (b). Shifting of STE nearest neighbors from their perfect positions exceeds 3% of lattice constant a. Oxygen O76 which carries a hole has the most noticeable displacement (excluding fictive atom "e" which represents the center of STE electron density. Table 2 and Table 3 demonstrate largest relaxations and spin charges in SC).

**Table 2.** Non-axial STE and surrounding atoms relaxations: top 10 of atoms with largest displacements. Displacements are denoted as Δ, measured in % of lattice constant a, spin charges are denoted as q. Correspondences between atomic numbers (at.#) and their positions in SC are shown in figure 1 (b)

| STE_in(x) | | | | | | STE_out(x) [a] | | |
|---|---|---|---|---|---|---|---|---|
| HF | | | B3LYP30 | | | HF | | |
| at.# | Δ, % | q, \|e\| | at.# | Δ, % | q, \|e\| | at.# | Δ, % | q, \|e\| |
| 109 | 36.05 | 1.356 | 109 | 35.47 | 1.499 | 109 | 36.34 | 1.339 |
| 76 | 22.98 | 0.753 | 76 | 22.47 | 0.595 | 76 | 24.12 | 0.765 |
| 31 | 8.580 | 0.098 | 31 | 7.893 | 0.098 | 22 | 8.756 | 0.009 |
| 22 | 7.599 | 0.009 | 22 | 7.365 | 0.006 | 32 | 6.896 | 0.051 |
| 85 | 7.159 | 0.100 | 85 | 7.079 | 0.137 | 33 | 6.896 | 0.051 |
| 83,84 | 3.720 | 0.002 | 23 | 3.406 | 0.002 | 31 | 6.891 | 0.008 |
| 7 | 3.222 | 0.001 | 83,84 | 2.241 | 0.002 | 82 | 4.669 | 0.044 |
| 23 | 3.193 | 0.000 | 7 | 2.769 | 0.001 | 86,87 | 3.632 | 0.067 |
| 32 | 3.156 | 0.008 | 82 | 2.269 | 0.002 | 55 | 2.738 | 0.005 |

[a] B3LYP30 did not give stable solution corresponding to STE_out(x) orientation.

**Table 3.** Axial STE and surrounding atoms relaxations: top 10 of atoms with largest displacements. Displacements are denoted as Δ, measured in % of lattice constant a, spin charges are denoted as q. Correspondences between atomic numbers (at.# ) and their positions in SC are shown in figure 1 (b)

| STE_in(z) | | | | | | STE_out(z) | | | | | |
|---|---|---|---|---|---|---|---|---|---|---|---|
| HF | | | B3LYP30 | | | HF | | | B3LYP30 | | |
| at.# | Δ,% | q,\|e\| | at.# | Δ,% | q,\|e\| | at.# | Δ,% | q,\|e\| | at.# | Δ,% | q,\|e\| |
| 109 | 29.659 | 1.540 | 109 | 25.635 | 1.385 | 109 | 35.94 | 1.523 | 109 | 46.644 | 1.417 |
| 76 | 21.177 | 0.576 | 76 | 21.958 | 0.400 | 76 | 18.10 | 0.557 | 76 | 14.866 | 0.431 |
| 22 | 8.024 | 0.109 | 22 | 8.122 | 0.103 | 22 | 12.97 | 0.011 | 22 | 10.390 | 0.001 |
| 82 | 4.642 | 0.069 | 82 | 3.817 | 0.033 | 31 | 5.223 | 0.015 | 23 | 6.407 | 0.019 |
| 83 | 4.642 | 0.069 | 83 | 3.817 | 0.033 | 32 | 5.223 | 0.015 | 85 | 4.479 | 0.019 |
| 84 | 4.642 | 0.069 | 84 | 3.817 | 0.033 | 33 | 5.223 | 0.015 | 86 | 4.479 | 0.019 |
| 31 | 4.594 | 0.009 | 31 | 3.509 | 0.005 | 23 | 4.691 | 0.014 | 87 | 4.479 | 0.021 |
| 32 | 4.594 | 0.009 | 32 | 3.509 | 0.005 | 85 | 4.339 | 0.084 | 31 | 3.364 | 0.108 |
| 33 | 4.594 | 0.009 | 33 | 3.509 | 0.005 | 86 | 4.339 | 0.084 | 32 | 3.364 | 0.108 |
| 23 | 3.289 | 0.003 | 85 | 3.098 | 0.003 | 87 | 4.339 | 0.084 | 33 | 3.364 | 0.108 |

*3.3. Electronic properties*

Partial density of states (DOS) diagrams of STE components are shown in figure 2 and figure 3. Electron and hole levels are distinctly located in energy gap. Localized hole state splits from VB by 6.4 eV for HF and 1.0 eV for B3LYP30 as to STE_out(z) and by 13.7 eV for HF and by 3.7 eV for B3LYP30 as to STE_in(z). STE electron level is splitted off from CB bottom by 10.7 eV for HF and by 3.8 eV for B3LYP30 as to STE_out(z) and by 10.4 eV for HF and by 3.6 eV for B3LYP30 as to STE_in(z).

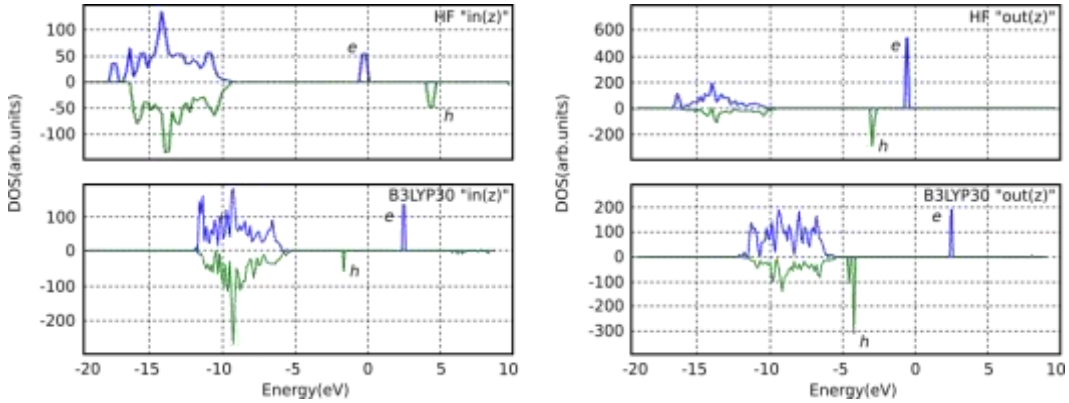


**Figure 2.** Density of states (DOS) diagrams for alpha (upper curves) and beta (lower curves) spin components of axial STE in beryllium oxide. Fermi level is at 0 eV.

Non axial STE is in conformable situation. Localized hole state splits off from a VB top by 13.8 eV for HF and 3.8 eV for B3LYP30 as to STE_in(x) and by 13.7 eV for HF as to STE_out(z). STE electron level is spitted off from CB bottom by 10.9 eV for HF and 4.0 eV for B3LYP30 as to STE_in(z) and by 11.7 eV for HF as to STE_out(z).

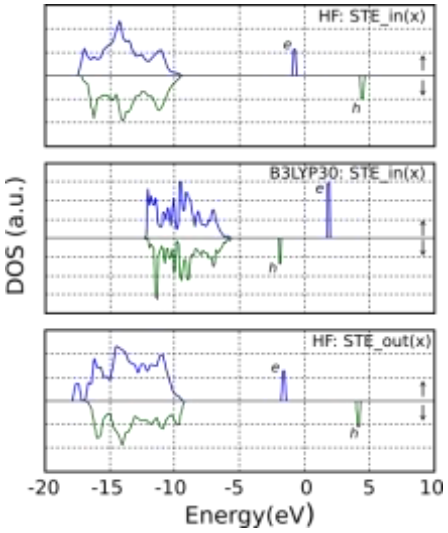


**Figure 3.** Density of states (DOS) diagrams for alpha (upper curves) and beta (lower curves) spin components of STE in beryllium oxide. Fermi level is at 0 eV.

Presence of two defect levels becomes apparent at luminescence spectrum also. STE triplet luminescence energies as a result of transition from low excited triplet state to ground state are given in Table 4 and Table 5. They were calculated using the ΔSCF method as the difference between the total energy of the fully relaxed triplet state and the ground singlet state at the triplet geometric structure. HF has better agreement with experimental data.

**Table 4**. STE(z) luminescence bands and α-parameter for exponent describing STE electronic component (SC 109 atoms)

| Config. | Parameter | HF | B3LYP30 | Exp.[5,6] |
|---|---|---|---|---|
| **STE_in(z)** | Elum | 6.0 | 6.5 | 4.9 |
| | α | 0.11 | 0.12 | - |
| **STE_out(z)** | Elum | 9.2 | 7.8 | 6.7 |
| | α | 0.11 | 0.11 | - |

**Table 5**. STE(x) luminescence bands and α-parameter for exponent describing STE electronic component (SC 109 atoms)

| Config. | Parameter | HF | B3LYP30 | Exp.[5,6] |
|---|---|---|---|---|
| **STE_in(x)** | Elum | 5.5 | 6.2 | 4.9 |
| | α | 0.12 | 0.10 | - |
| **STE_out(x)** | Elum | 4.7 | -* | 4.4 |
| | α | 0.12 | -* | - |

HF shows a reversed position of defect levels and overestimates Eg extent. Nevertheless, it gave reasonable results for all luminescence peaks under consideration (an average inaccuracy of 20%). Hybrid functional B3LYP30 have more noticeable deviation (25%) and did not give stable solution for one of the configurations (STE_out(x)). Divergence of STE_out(x) could be connected with its less tight site space for STE electron and excessive delocalization of electron over it.

## 4. Conclusions

In this paper, we have presented the results of STE computation modelling in BeO intended for better understanding of these type electronic excitations. It could be also interested from an aspect of modern methods application especially taking into consideration lack of theoretical investigation results relevant to STE in beryllia. Comparison of B3LYP functional with non-standard 30% of exact exchange and pure HF approach was done in the context of STE modelling in BeO crystal. B3LYP30 have advantages as to perfect crystal, but for some luminescence bands of STE it appears to be quantitatively less accurate than HF, in spite of correct relative position of defect levels. Calculated data for STE triplet luminescence reasonably agree with the experimental one.

## 5. References

[1] Knox R S 1963 *Theory of excitons, Solid state physics* (Ed. by Seitz and Turnbul, Academic, New York) **5**
[2] Lushchik Ch B 1985 *Excitons* (Moscow, Nauka) pp 362–385
[3] Song RT and. Williams R T 1993 *Self-Trapped Excitons* (Springer-Verlag, Berlin Heidelberg New York)
[4] Itoh N and Stoneham A M 2003 *Materials Modification by Electronic Excitation* (Cambridge University Press)
[5] Giniyatulin K N, Malysheva A F, Kruzhalov A V and Kyarner T N1982 *Tr.Inst.Fiz.Akad.Nauk Estonii* **53** 71
[6] Ivanov V Y, Pustovarov V A, Kruzhalov A V and Shulgin B V 1989 *Nucl. Instr. Meth. Phys. Res. A* **282** 559
[7] Gorbunov S V, Yakovlev V Yu, Ivanov V Yu and Kruzhalov A V 1990 *Soviet Physics – Solid State* **32** 10 1708
[8] Tausenev D S, Milman I I, Ivanov V Yu and. Kruzhalov A V 2008 *Radiation Measurements* **43** pp 349 – 352
[9] Kislov A N , Kruzhalov A V , Varaksin A N and Mazurenko V G 1991 *Soviet Physics – Solid State* **33** 10 1659
[10] Dovesi R, Sounders V R, Roetti C *et al* 2013 *CRYSTAL09 User's Manual* (University of Tourino)
[11] Becke A D 1993 *J.Chem.Phys.* **98** 7 5648-5652
[12] Stephens P J, Devlin F J, Chablowski C F and Frish M J 1994 *J.Phys.Chem.* **98** 45 11623-11627
[13] Lichanot A, Chaillet M, Larrieu C, Dovesi R and Pisani C 1992 *Chem. Phys.* **164** 383-394
[14] Towler M D, Allan N L, Harrison N M, Saunders V R, Mackrodt W C and Apra E 1994 *Phys. Rev. B* **50** 5041-5054

[15] Anderson D G 1964 *J. Assoc. Comput. Mach.* **12** 547
[16] Ramo D M, Sushko P V and Shluger A L 2012 *Phys.Rev.B* **85** 024120
[17] Shluger A L and Stefanovich E V 1990 *Phys.Rev.B* **42** 9664
[18] Gavartin J L and Shluger A L2001 *Phys.Rev.B* **64** 245111
[19] Kuznetsov A Y , Sobolev A B , Makarov A S and Botov M A 2009 *Russian Physics Journal*, **52** 8/2 83
[20] Kuznetsov A Yu, Botov M A, Makarov A S and Sobolev A B2014 *Russian Physics Journal*, **57** 12-3 36
[21] Martienssen W and Warlimont H (Eds.) 2005 *Springer Handbook of Condensed Matter and Materials Data* (ISBN 3-540-44376-2 Spinger Berlin Heidelberg New York)
[22] Hazen R M and Finger L W1986 *J.Appl.Phys.* ***59*** 3728